



OPEN

Green synthesis of zinc oxide nanoparticles using Sea Lavender (*Limonium pruinosum* L. Chaz.) extract: characterization, evaluation of anti-skin cancer, antimicrobial and antioxidant potentials

Bassant Naïel ¹✉, Manal Fawzy ^{1,2,3}, Marwa Waseem A. Halmy ¹ & Alaa El Din Mahmoud ^{1,2}

In the present study, a green, sustainable, simple and low-cost method was adopted for the synthesis of ZnO NPs, for the first time, using the aqueous extract of sea lavender, *Limonium pruinosum* (L.) Chaz., as a reducing, capping, and stabilizing agent. The obtained ZnO NPs were characterized using ultraviolet–visible spectroscopy (UV–VIS), Fourier transform infrared spectroscopy (FT-IR), scanning electron microscopy (SEM), energy-dispersive X-ray analysis (EDX), transmission electron microscopy (TEM), X-ray diffraction (XRD) and thermogravimetric analysis (TGA). The UV–Vis spectra of the green synthesized ZnO NPs showed a strong absorption peak at about 370 nm. Both electron microscopy and XRD confirmed the hexagonal/cubic crystalline structure of ZnO NPs with an average size ~ 41 nm. It is worth noting that the cytotoxic effect of the ZnO NPs on the investigated cancer cells is dose-dependent. The IC₅₀ of skin cancer was obtained at 409.7 µg/ml ZnO NPs. Also, the phyto-synthesized nanoparticles exhibited potent antibacterial and antifungal activity particularly against Gram negative bacteria *Escherichia coli* (ATCC 8739) and the pathogenic fungus *Candida albicans* (ATCC 10221). Furthermore, they showed considerable antioxidant potential. Thus, making them a promising biocompatible candidate for pharmacological and therapeutic applications.

With the increasing demand for waste minimization and achieving sustainable development goals through the adoption of the fundamental principles of green chemistry, there is an obvious need for alternative green methods for nanoparticles synthesis^{1,2}.

The adoption of green processes in different technologies has been increasingly widespread and is becoming necessary as a result of global environmental problems associated with harsh conventional chemical and physical processes^{3–6}.

Nanotechnology has drawn more attention for its cutting-edge nature and wide application range in almost every field of science and technology including biomedical sciences^{7,8}. Generally, nanoparticles (NPs) are manufactured using several chemical and physical methodologies, which are quite expensive and pose risks to the environment and human health^{6,9–11}.

Plants are the most preferred green and facile route for the synthesis of nanoparticles as they promote large-scale production of stable nanoparticles of various shapes and sizes. Using natural plant extracts is an eco-friendly, simple and cost-effective approach^{12,13}. Plant extracts may contain phytochemical compounds such as

¹Environmental Sciences Department, Faculty of Science, Alexandria University, Alexandria 21511, Egypt. ²Green Technology Group, Faculty of Science, Alexandria University, Alexandria 21511, Egypt. ³National Biotechnology Network of Expertise (NBNE), Academy of Scientific Research and Technology (ASRT), Cairo, Egypt. ✉email: bassant_hassan22@yahoo.com

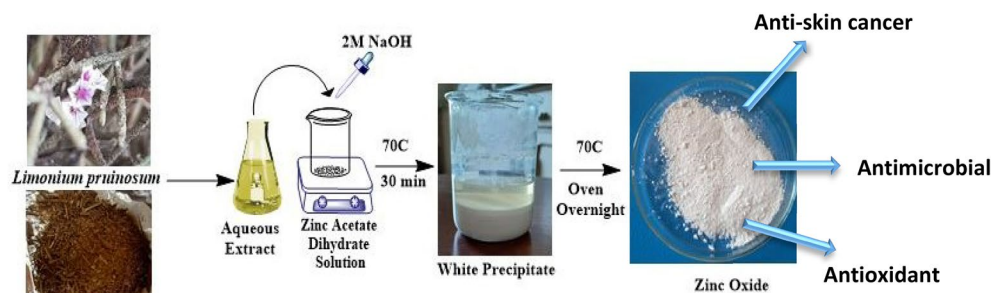


Figure 1. Schematic illustration of the phytosynthesis of ZnO NPs.

phenols, flavonoids, alkaloids, terpenes, saponins, and tannins that play as both reducing agents and capping or stabilization agents^{14–16}.

Among nanometal oxides, ZnO NPs are known for their antimicrobial¹⁷, anti-inflammatory and anticancer activity^{12,18,19}. They are also used in sunscreens due to their characteristic ultraviolet ray scattering properties^{20,21}, drug delivery^{22,23}, and wound-healing applications^{24,25}. ZnO NPs have several properties as biocompatible multifunctional nanomaterial. The U.S. Food and Drug Administration (FDA) identifies ZnO as a so-called GRAS (= generally recognized as safe) substance²⁶. Several studies have demonstrated approaches for the green synthesis of zinc oxide nanoparticles using different plant extracts^{17,19,27,28}. However, the sea lavender plant, *Limonium pruinosum* (L.) Chaz., has not been reportedly used for ZnO NPs Synthesis. *Limonium pruinosum* is a halophytic plant that belongs to family Plumbaginaceae. It is a non-succulent, salt excretive, subshrub which lives in two different habitats, coastal salt marsh and desert limestone cliffs²⁹.

In the last decade, some plant species has been investigated for their role in the synthesis of nanoparticles^{30–33}. However, halophytic and salt marsh dwelling plants have received little attention regarding their potentials for the synthesis of nanoparticles.

Globally, salt marshes provide key ecosystem services contributing several economic, social and ecological aspects^{34–36}. Salt marshes are among the most significant blue carbon ecosystems, having a vital role in carbon sequestration, lowering greenhouse gases, and mitigating climate change impacts. Unfortunately, they are vulnerable to severe degradation³⁷. Highlighting the resources and potential uses of the species in salt marshes can contribute to the conservation and restoration efforts of these valuable and undermined ecosystem. Therefore, the main objectives of this study are to assess the potentiality of a native salt marsh and common ornamental plant in the Mediterranean basin, *Limonium pruinosum*, for the phytosynthesis of ZnO NPs and the possible use of its aqueous extract and synthesized ZnO NPs in biomedical applications.

Material and methods

Collection and preparation of plant specimens. Plant specimens (Supplementary Fig. 1) were collected from their natural habitats, the salt marshes along the northwestern Mediterranean coast of Egypt, particularly from El-Alamein (Latitude 30° 55' 338", Longitude 28° 29' 365", Altitude 11). Plant material was collected in accordance with applicable national and international guidelines³⁸. Permission for collecting the investigated plant species for scientific purposes was obtained from Environmental Sciences Department, Alexandria University. Plant specimens were identified by Dr. Marwa Waseem A. Halmy according to Boulos³⁹. Voucher specimens were deposited in Tanta University Herbarium (TANE) with voucher Numbers: 14200–14210, which is a public herbarium providing access to the deposited material. The shoot system, leaves and stems, were utilized in this investigation. Specimens were carefully washed using tap water then distilled water, to remove soil particles. Afterward, the specimens were dried at 60 °C to constant weight then grounded to fine powder using a stainless-steel grinder Moulinex 700 W, France. Plant powder was preserved in airtight jars for subsequent use.

Preparation of plant extract. Two grams of plant powder were stirred and heated at 70 °C in 100 ml distilled water for 30 min. The extract was allowed to cool to room temperature. The pH of plant extract was 7.84. The extract was filtered using Whatman filter paper No.1 and stored at 4 °C for subsequent experimental use.

Green synthesis of ZnO NPs. Zinc acetate dihydrate {Zn (CH₃COO)₂·2H₂O} and Sodium Hydroxide (NaOH) were purchased from Loba Chemie, India.

Briefly, 2.5 ml of plant extract was added to 25 ml 0.5 M Zinc acetate dihydrate. The pH of the mixture was 6.13, 2 M NaOH was added drop wise to maintain pH at 8, then the mixture was then stirred and heated at 70 °C for 30 min for complete reduction and formation of a white precipitate.

The resulting material was then collected via decantation, washed with distilled water to remove residuals and oven dried at 70 °C for overnight to yield powdered ZnO nanoparticles^{17,40,41}. The synthesis steps are demonstrated in Fig. 1. The dried sample was stored at room temperature in airtight container for further characterization and applications. The yield percentage was then estimated according to the following formula:

$$\text{Yield(\%)} = (\text{Experimental weight of ZnO} / \text{Theoretical weight of ZnO}) \times 100 \quad (1)$$

Characterization of ZnO NPs. The synthesized ZnO NPs from the aqueous extract of *L. pruinosum* were confirmed and characterized using double-beam UV–visible spectrophotometer (T70/T80 series UV/Vis Spectrophotometer, PG Instruments Ltd, U.K.) in the range of 200–800 nm to observe the characteristic peak confirming ZnO NPs formation.

Fourier transform infrared spectroscopy (FT-IR) (Nicolet iS50 FTIR Spectrometer, Thermo Fischer Scientific, Japan) in the range of 4000–400 cm^{-1} and gas chromatography–mass spectrometry (GC–MS) (Trace GC1310-ISQ mass spectrometer, Thermo Scientific, Austin, TX, USA) were both used for the determination of the functional groups and phytoconstituents contributing to the reduction and stabilization of the ZnO NPs. Scanning electron microscope, energy dispersive X-ray analysis (EDX) using (JEOL, JSM IT 200, Japan), transmission electron microscope using (JEOL, JSM-1400 PLUS, Japan) and X-ray diffractometer (Bruker D8 Discover Diffractometer, USA) were used to analyze the surface morphology, identify the elemental composition, size, and shape of green synthesized ZnO NPs. Moreover, thermogravimetric analysis was conducted using Labsys evo Setaram, France, for the determination of the thermal stability of the green synthesized ZnO NPs.

Anti-skin cancer/cytotoxicity. Evaluation of cell viability for green synthesized ZnO NPs was performed using MTT assay against A-431 (Skin cancer/Epidermoid Carcinoma) and WI-38 (Normal lung fibroblast cells); purchased from Vacsera center, Giza, Egypt; at different concentrations of ZnO NPs and *L. pruinosum* extract (31.25, 62.5, 125, 250, 500 and 1000 $\mu\text{g}/\text{ml}$). Methylthiazolyl diphenyl-tetrazolium bromide (MTT) assay is the most commonly used method for assessing metabolic activity of cells. It is a reliable colorimetric and quantitative assay based on the ability of the cellular mitochondrial dehydrogenase enzyme to cleave the yellow water soluble MTT to produce insoluble dark blue/purple formazan deposits in living cells used⁴².

Briefly, a 96-wells tissue culture plate was inoculated with 1×10^5 cells/ml (100 μl /well) and incubated at 37 °C for 24 h. Growth medium was then decanted. Two-fold dilutions of the tested sample were preserved in RPMI medium with 2% serum. The wells were treated using 0.1 ml of each dilution and 3 wells were used as control, receiving only serum. The plate was incubated at 37 °C and then examined. Morphological changes of cells were investigated. MTT solution was prepared (5 mg/ml in PBS) (BIO BASIC CANADA INC). About 8–20 μl of MTT solution were added to each well, thoroughly shaken for 5 min, and incubated (37 °C, 5% CO_2) for 4 h till formation of formazan. After that, formazan was resuspended in 200 μl DMSO and shaken thoroughly for 5 min. Absorbance was measured at 560 nm^{43–45}. Experiment was performed in triplicate. The concentration of ZnO NPs and *L. pruinosum* extract required to inhibit the growth of the skin cancer cells (A-431) by half was calculated from the dose–response curve and represented as IC_{50} .

Antimicrobial activity. The antimicrobial activity of green synthesized ZnO NPs, *L. pruinosum* extract, and Gentamycin was tested against 6 different pathogenic microorganisms including Gram positive bacteria (*Bacillus Subtilis* (ATCC 6633), *Staphylococcus aureus* (ATCC 6538)), Gram negative bacteria (*Escherichia coli* (ATCC 8739), *Enterobacter aeruginosa*) and pathogenic fungi (*Candida albicans* (ATCC 10221) and *Aspergillus flavus*).

Antimicrobial activity was determined by using the agar well diffusion method^{46,47}. Ten mg/ml of all samples were dissolved in normal saline (0.9% NaCl). Saline did not have antimicrobial activity against all tested pathogenic strains. Gentamycin was tested as a positive control. One hundred μl of green synthesized ZnO NPs, *L. pruinosum* extract, and Gentamycin was tested.

Antioxidant activity. Antioxidant activity of green synthesized ZnO NPs and *L. pruinosum* extract were determined using 2,2-diphenyl-1-picrylhydrazyl (DPPH) assay. In brief, 1 ml of 0.1 Mm DPPH solution was added to 3 ml of green synthesized ZnO NPs and plant extract in ethanol at different concentrations (1.95, 3.9, 7.8125, 15.625, 31.25, 62.5, 125, 250, 500, 1000 $\mu\text{g}/\text{ml}$). These concentrations were prepared by dilution method. Ascorbic acid was used as standard. The control DPPH was measured without sample. The mixture was shaken vigorously and allowed to stand at room temperature for 30 min. In order to measure the absorbance a spectrophotometer (UV–VIS Milton Roy, USA) was used at 517 nm. The assay was conducted in triplicate. The IC_{50} value was calculated using Log dose inhibition curve. The percentage of DPPH scavenging effect was calculated using the following equation:

DPPH scavenging effect (%)^{16,30}:

$$A_0 - A_1/A_0 \times 100 \quad (2)$$

where A_0 was the absorbance of the control reaction and A_1 was the absorbance in the presence of test.

Results and discussion

Characterization of ZnO NPs. After the addition of plant extract to Zinc acetate dihydrate precursor and NaOH, white precipitate was formed indicating the phytofabrication of ZnO NPs with a yield equal to 88.2%. This finding supports large scale production of ZnO NPs using plant-mediated synthesis procedure close to chemical methods⁴⁸.

UV–Vis spectra analysis. The obtained ZnO NPs were suspended in deionized water and sonicated for 10 min to detect the UV–visible spectra. The UV–Vis spectra showed a strong absorption peak at about 370 nm confirming the successful formation of ZnO NPs using aqueous extract of *L. pruinosum*. Moreover, the UV–Vis spectra of plant extract showed absorption peak at 320 nm indicating the presence phenolic compounds as illustrated in Fig. 2a. This result is in agreement with other previous studies^{49–51}.

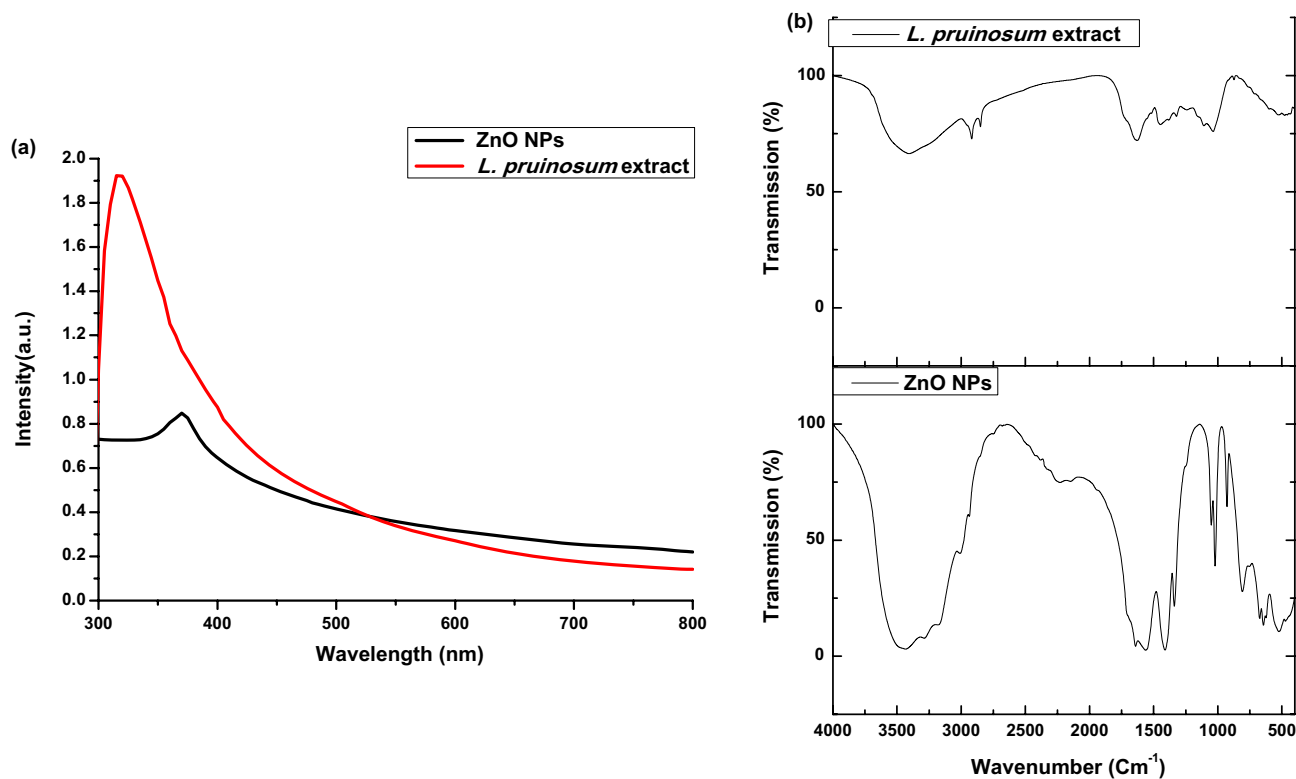


Figure 2. (a) UV-Vis spectrum; (b) FT-IR of *L. pruinosum* extract and the phytosynthesized ZnO NPs.

No.	Compound name	Chemical structure	Category	Retention time (min)	Area (%)
1	Carvone	$C_{10}H_{14}O$	p-Menthane Monoterpenoid	12.79	2.93
2	Bergamotol, Z-à-trans-	$C_{15}H_{24}O$	Sesquiterpenoid	19.72	6.13
3	6-epi-shyobunol	$C_{15}H_{26}O$	Sesquiterpenoid	23.09	11.51
4	Bisabolol oxide A	$C_{15}H_{26}O_2$	Oxanes	25.10	6.49
5	Hexadecanoic acid, TMS	$C_{19}H_{40}O_2Si$	Ester	31.29	11.67
6	Oleic Acid, (Z)-, TMS derivative	$C_{21}H_{42}O_2Si$	Ester	34.37	3.66
7	Monolinolein, TMS	$C_{27}H_{54}O_4Si_2$	Ester	37.93	2.16

Table 1. Bioactive compounds identified in aerial parts of *L. pruinosum* extract.

Fourier transform infrared spectroscopy (FT-IR). The FT-IR revealed the presence of a characteristic peak at about 523 cm^{-1} which indicated the formation of Zn-O nanostructure stretching similarly⁵². The vibrational peaks observed at around 3433 and 3288 cm^{-1} could be corresponding to hydroxyl (OH) groups which are observed at around 3407 of *L. pruinosum* and are possibly related to phenolic and alcoholic compounds. However, the peak projected around 2937 cm^{-1} corresponds to the C-H stretching. The peak at around 1050 cm^{-1} is corresponding to the stretching of the -CN group which was observed at around 1035 cm^{-1} of *L. pruinosum*.

In addition, the vibrational peaks at 1640 cm^{-1} and 1560 cm^{-1} were corresponding to the H-O-H bending as shown in Fig. 2b. Similarly, the H-O-H bending was observed at around 1630 cm^{-1} of *L. pruinosum*. The peaks mentioned above confirm the presence of phytochemicals such as terpenoids and phenolics in the plant extract that were involved in the reduction and stabilization of ZnO NPs. These results are supported by other previous findings^{18,53,54}. Moreover, plant extract is also further characterized using GC-MS to define the major compounds involved in the synthesis process.

Phytochemical screening. The phytochemical analysis of plant extract was carried out using GC-MS to determine phytochemicals that may be involved in the reduction and stabilization of ZnO NPs as presented in Supplementary Fig. 2 and Table 1. The identification of phytochemicals was conducted using WILEY 09 and NIST 11 mass spectral databases based on a comparison of their retention times and mass spectra^{55,56}.

Totally 7 major compounds were identified from GC-MS chromatogram belonging to different categories including p-menthane Monoterpenoid, Sesquiterpenoid, Oxanes, and Esters. The major constituents were Hexadecanoic acid, TMS (11.67%), 6-epi-shyobunol (11.51%), Bisabolol oxide A (6.49%), Bergamotol, Z-à-trans- (6.13%), Oleic Acid, (Z)-, TMS derivative (3.66%), Carvone (2.93%) and Monolinolein, TMS (2.16%)

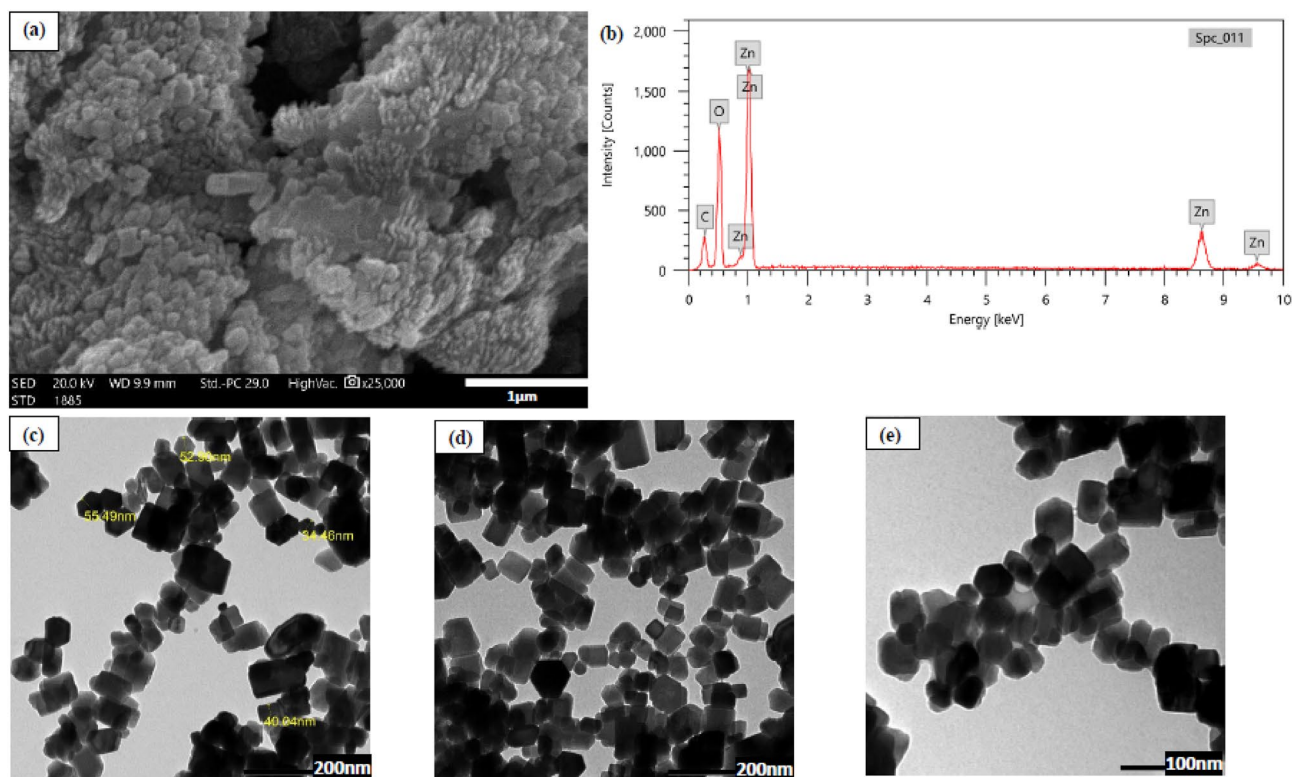


Figure 3. (a) SEM; (b) EDX; (c–e) TEM images of the phytosynthesized ZnO NPs.

Plant species	Shape	Size (nm)	References
<i>Artocarpus gomezianus</i> Wall. ex Trécul	Spherical	10–30	60
<i>Berberis aristata</i> DC	Needle	20–40	61
<i>Artocarpus heterophyllus</i> Lam	Spherical	12–24	62
<i>Prosopis farcta</i> (Banks & Sol.) J.F. Macbr	Hexagonal	40–50	63
<i>Phoenix dactylifera</i> L	Spherical	22	64
<i>Avena Sativa</i> L	Hexagonal	100	65
<i>Limonium pruinatum</i> (L.) Chaz	Hexagonal/cubic	~41	Present study

Table 2. Comparison of biosynthesized ZnO NPs using different plant species.

in descending order of percentage. These phytochemicals may be incorporated in the phyto-reduction of nanoparticles^{57,58}.

Based on UV–Vis, FT-IR and GC–MS results it can be concluded that *L. pruinatum* extract consists of several phytochemicals including; alcohols, phenols, terpenoids and esters which acted as reducing and stabilizing agent for successful phytosynthesis of ZnO NPs.

Morphological structure. Scanning electron microscope (SEM), energy dispersive X-ray analysis (EDX), and transmission electron microscope (TEM) were used to analyze the surface morphology, size, and shape of green synthesized ZnO NPs as illustrated in Fig. 3.

Figure 3 a shows that the obtained ZnO NPs are crystalline in nature. The EDX results confirmed the purity of the obtained ZnO NPs and the presence of Zinc in its oxide form as shown in Fig. 3b. Strong emission peaks of Zn were detected at ~1 keV, 8.6 keV and 9.6 keV. The detected emission peaks of carbon at ~0.3 keV and oxygen at ~0.5 keV might be due to the plant biomass used in phyto-synthesis. These findings are consistent with that of Barzinjy and Azeez⁵⁹. The TEM images showed the hexagonal/cubic shape of green synthesized ZnO NPs with an average size of ~41 nm as shown in Fig. 3c–e. Several studies reported various shapes and size of the biosynthesized ZnO NPs as illustrated in Table 2.

X-ray diffraction (XRD). Dried ZnO NPs were used for XRD analysis with Cu-K α radiation ($\lambda = 1.54060 \text{ \AA}$), the relative intensity data were collected over a 2θ range of 5–100 degrees. The XRD pattern of ZnO NPs (Fig. 4a) reveals sharp peaks that indicate the purity and crystallinity of green synthesized ZnO NPs. The 2θ angles of the

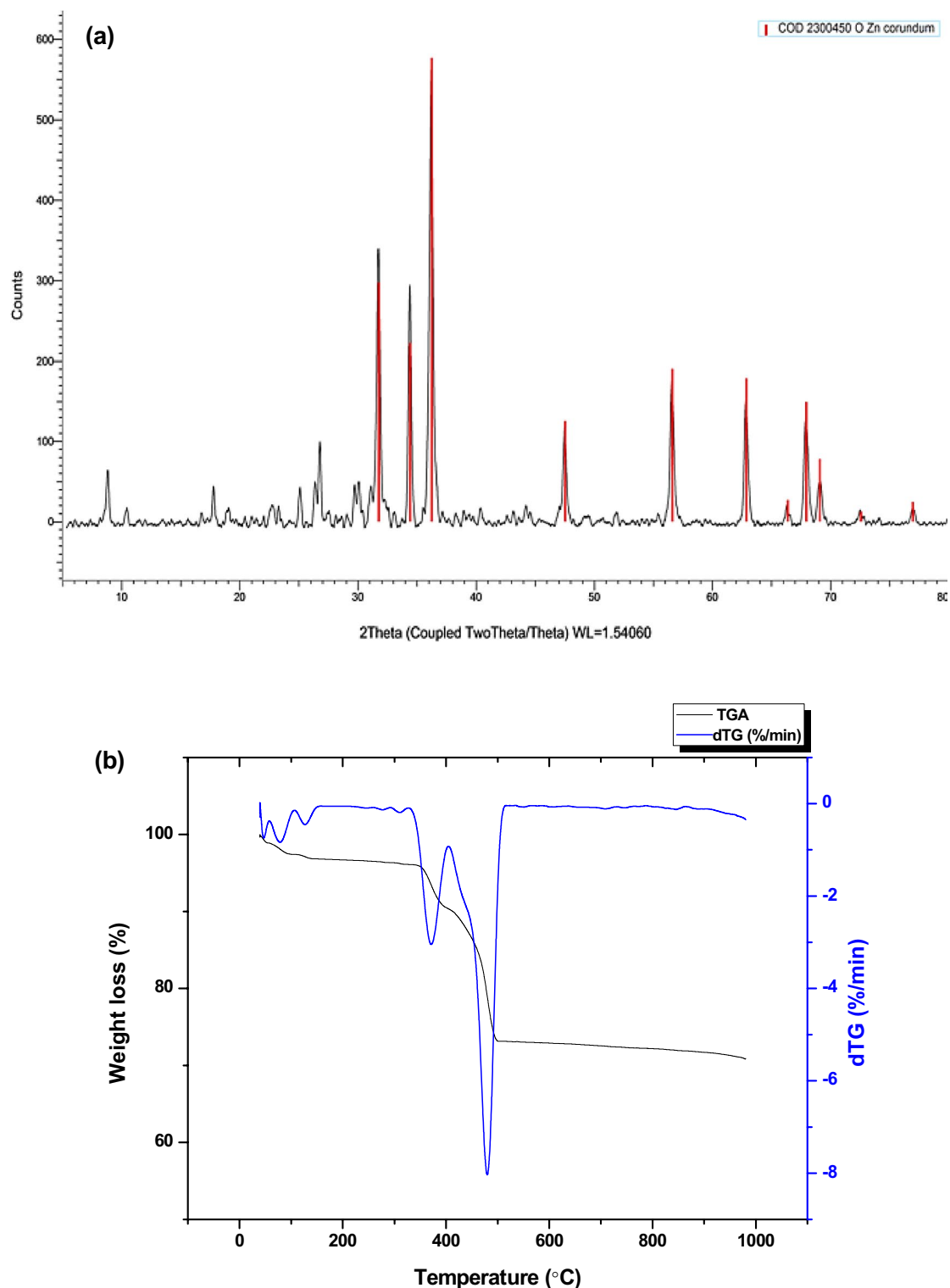


Figure 4. (a) XRD pattern and (b) TGA pattern of the phytosynthesized ZnO NPs.

diffraction peaks were located at $\sim 31.45^\circ$, 34.66° , 36.26° , 47.48° , 56.29° , 62.7° , and 68.31° . These peaks are similar to those reported in other studies^{47,59}.

The peaks were paralleled to JCPDS Card (2300450) confirming the hexagonal phase of ZnO NPs with space group P 63 mc (186). XRD analysis detected the average crystalline size of obtained ZnO NPs ~ 11 nm using Debye–Scherrer's equation⁶⁶.

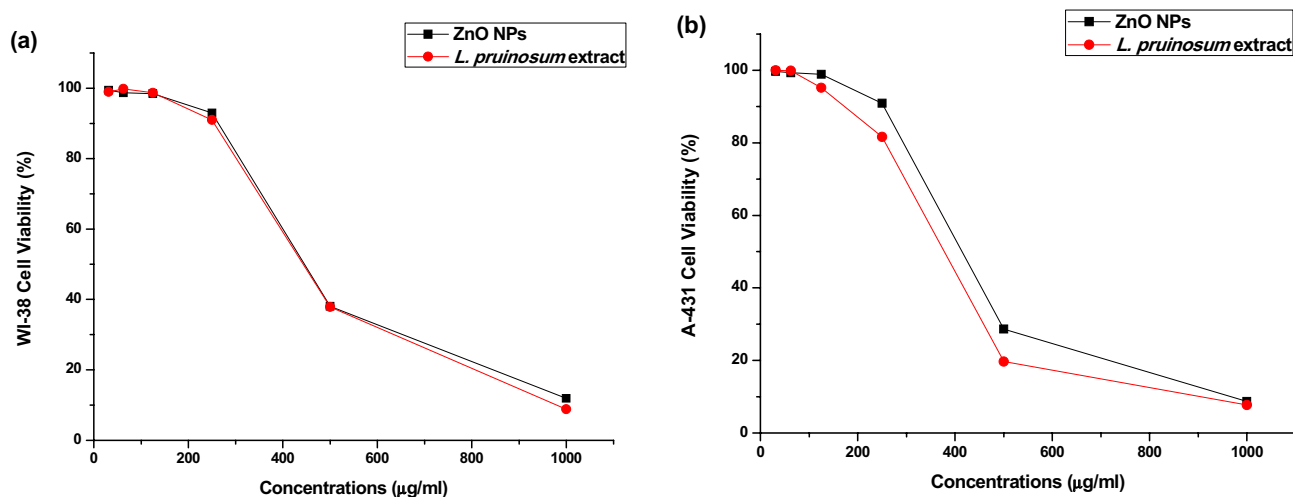


Figure 5. Cell viability % efficiency of the phytosynthesized ZnO NPs and *L. pruinosa* extract against (a) normal lung fibroblast cells (WI-38) and (b) cancerous cells (A-431).

Size difference between XRD and above-mentioned TEM was possibly attributed to the fact that XRD gives information about the grain size and larger particles may be polycrystalline as a result of the coalescence of smaller grains^{67,68}.

Thermogravimetric analysis (TGA). The thermogravimetric analysis was conducted using (Labsys evo Setaram, France) for the determination of thermal stability of green synthesized ZnO NPs as shown in Fig. 4b. The weight loss of the ZnO NPs dried powder was measured while subjected to thermal fluctuations from room temperature to 1000 °C. The heating was carried out under Nitrogen atmosphere with temperature scanning rate 10 °C/min.

It was shown that the green synthesized ZnO NPs exhibited a high thermal stability. As a gradual weight loss up to about 29.08% of actual weight at the temperature range from room temperature to 1000 °C, which is likely due to loss of moisture content and organic substances in the samples^{27,33,54}.

In contrast, Barzinjy and Azeez⁵⁹ observed a considerable weight-loss (~65%) between 350 and 600 °C, which was attributed to the degradation of organic groups involved in the biosynthesis of ZnO NPs using plant extract. These results indicated that the plant-mediated synthesis of ZnO NPs was thermally stable.

Anti-skin cancer/cytotoxicity. The MTT assay results demonstrated that cancer cell viability decreased significantly to 28.6% at 500 µg/ml of ZnO NPs after 24 h exposure. The anticancer activity of ZnO NPs exhibited dose-dependent profile as shown in Fig. 5 in agreement with previous studies^{69,70}.

The outcomes were in accordance with that of the study conducted by Nilavukkarasi et al.¹² that examined lung cancer cell lines (A549) using cell proliferation assay at different concentrations (1.45, 3.9, 7.8, 15.6, 31.2, 62.5, 125, 250, and 500 µg/ml) of synthesized ZnO. Major alterations of cells were observed at higher concentrations such as cell shrinkage and extensive cell detachment, which is consistent with the outcomes of the current study as shown in Supplementary Fig. 3a,b.

The concentration of ZnO NPs required to inhibit the growth of the skin cancer cells (A-431) by half calculated from the dose–response curve $IC_{50} = 409.7$ µg/ml. Lingaraju et al.⁷¹ have reported that the (IC_{50}) was found to be 383.05 µg/ml and 329.67 µg/ml for lung (A549) and Hepatocarcinoma (HePG2) cell lines, respectively.

The green synthesized ZnO NPs in the current study showed higher toxicity towards cancer cells compared to normal cells (WI-38), IC_{50} of ZnO NPs was 568.59 and 409.7 µg/ml against normal cells and cancerous cells, respectively.

Based on previous studies, green synthesized ZnO NPs showed high biocompatibility and less toxicity towards normal cells⁷. For instance, the green synthesized ZnO NPs using *Crotalaria verrucosa* leaf extract was tested against HeLa and DU145 cell lines and cytotoxicity assay revealed its selectivity for cancer cells highlighting its potential as substitute therapy against cervical and prostate cancer⁷².

The possible mechanism of anticancer effect of ZnO NPs may be attributed to oxidative stress and apoptosis^{62,73}.

Anticancer activity of *L. pruinosa* extract was also examined and the results demonstrated that plant extract showed higher activity than green synthesized ZnO NPs, the IC_{50} of plant extract was 554.17 and 362.74 µg/ml against normal cells and cancerous cells respectively as shown in Fig. 5a,b and confirmed by microscopic examination as shown in Supplementary Fig. 3a,b. This may be attributed to phytochemical content of *L. pruinosa* species particularly Hexadecanoic acid, as it has been known that these compounds may have the ability to halt cancer cell growth^{74–77}. Several previous studies also confirmed the potential anticancer activity of green synthesized ZnO NPs and plant phytochemicals^{63,78,79}. Furthermore, based on our investigation, both *L. pruinosa* extract and its green synthesized ZnO NPs showed no cytotoxic effect on normal cells (WI-38) up to 250 µg/ml compared to studies performed by Jobie et al.⁸⁰ and Chen et al.⁸¹ who observed that ZnO NPs are toxic to normal

Pathogenic microorganism	Limonium	ZnO NPs	Control (gentamicin)
<i>Bacillus subtilis</i> (ATCC 6633)	20	24	22
<i>Staphylococcus aureus</i> (ATCC 6538)	24	26	15
<i>Escherichia coli</i> (ATCC 8739)	31	29	17
<i>Enterobacter aeruginosa</i>	16	20	16
<i>Candida albicans</i> (ATCC 10221)	29	28	23
<i>Aspergillus flavus</i>	11	14	20

Table 3. Inhibition zones (diameter in mm) of phytosynthesized ZnO-NPs and *L. pruinorum* extract against different pathogenic microorganisms.

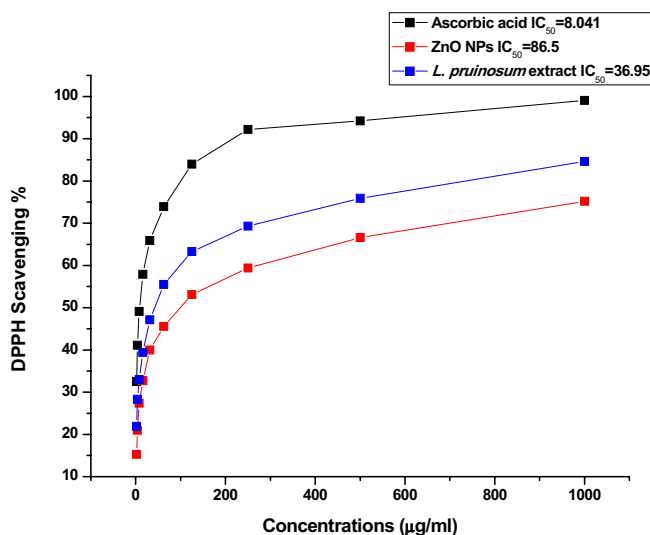


Figure 6. Antioxidant activity of ZnO NPs, *L. pruinorum* extract and Ascorbic acid.

vero cells at concentrations of 120 and 100 µg/ml, respectively. These findings suggest the high biocompatibility of *L. pruinorum* extract and ZnO NPs.

Antimicrobial activity. The results of antimicrobial activity of green synthesized ZnO NPs, *L. pruinorum* extract and Gentamycin tested against six different pathogenic microorganisms are shown in Table 3.

The results revealed that the synthesized ZnO NPs and plant extract showed the highest inhibition zone versus *E. coli* with 29 and 31 mm followed by *C. albicans* with 28 and 29 mm, respectively. Plant extract and its green synthesized ZnO NPs exhibited strong antimicrobial activity over conventional antibiotic Gentamycin except for *A. flavus*. It has been previously reported that ZnO NPs have significant antimicrobial activity^{40,79,82,83}. Antimicrobial activities of halophytes were attributed to phenolics due to their hydroxyl functional groups, degree of polymerization and lipophilicity; enhancing their binding to bacterial cell membrane as extensively discussed studies^{84,85}. Guimarães et al.⁸⁶ also investigated the antibacterial mechanism of action of phytochemicals and it was attributed to disruption of cellular membrane and eventually cell death. The mechanism of action of ZnO NPs depends on binding and interacting to the cell membrane and accumulation in the lipid layer leading to inhibition of enzymes, DNA and ATP synthesis promoting cell lysis¹⁷. Moreover, Soltanian et al.⁴¹ and Sirelkhatim et al.⁸⁷ demonstrated that ZnO NPs induce excessive reactive oxygen species generation and cell wall damage.

Antioxidant activity. The results presented in Fig. 6 revealed that ZnO NPs exhibited considerable antioxidant activity via the scavenging of free radicals⁸⁸ in a dose-dependent manner⁸⁹. The highest DPPH activity was recorded at 1000 µg/ml as 75.2% for ZnO NPs and 84.6% for *L. pruinorum* extract. In the present study the IC₅₀ of ZnO = 86.5 µg/ml, whereas Loganathan et al.¹⁵ have reported IC₅₀ = 95.80 µg/ml. *L. pruinorum* extract showed relatively higher antioxidant activity than their phyto-synthesized ZnO NPs due to the presence of secondary metabolites as confirmed by FT-IR and GC-MS results. For instance, phenolics and terpenoids are potent antioxidants. These phytochemicals also acted as capping agent for ZnO NPs and possibly related to their antioxidant activity⁹⁰. Moreover, Lopes et al.⁸⁴ and Bose et al.⁹¹ demonstrated that halophytes have high antioxidant capability to tolerate salinity stress and rich in phenolic content with remarkable antioxidant activity.

Conclusion

The current study demonstrated the efficiency of the aqueous extract of sea lavender, *Limonium pruinosum*, as reducing, capping and stabilizing agent leading to the successful synthesis of hexagonal/cubic zinc oxide nanoparticles. To the best of our knowledge, this study is the first to report the green synthesis of ZnO NPs using the aqueous extract of this halophytic plant species and the use of zinc acetate dihydrate as a precursor. The green synthesized ZnO NPs exhibited considerable anticancer activity against A-431 cell lines. Both plant extract and its green synthesized ZnO NPs showed no cytotoxic or detrimental effect on normal cells (WI-38) up to 250 µg/ml supporting its biocompatibility. Also, ZnO NPs along with plant extract exhibited remarkable antimicrobial activity compared to Gentamycin. Moreover, they showed comparable antioxidant activity. These findings suggest the adoption of *Limonium pruinosum* ZnO NPs as cost effective and ecofriendly candidate for biomedical and therapeutic applications. The present study adds more support for the urgent need for the conservation and sustainable management of salt marshes ecosystems and its halophytic plant species not only for their undeniable role in carbon sequestration but also as a sustainable resource for green synthesis of nanomaterials.

Data availability

All data generated or analyzed during this study are included within the article.

Received: 7 October 2022; Accepted: 21 November 2022

Published online: 27 November 2022

References

1. Becker, J., Manske, C. & Randl, S. Green chemistry and sustainability metrics in the pharmaceutical manufacturing sector. *Curr. Opin. Green Sustain. Chem.* <https://doi.org/10.1016/j.cogsc.2021.100562> (2022).
2. Rajasekharreddy, P., Rani, P. U. & Sreedhar, B. Qualitative assessment of silver and gold nanoparticle synthesis in various plants: A photobiological approach. *J. Nanoparticle Res.* **12**, 25 (2010).
3. Mahmoud, A. E. D. Eco-friendly reduction of graphene oxide via agricultural byproducts or aquatic macrophytes. *Mater. Chem. Phys.* **253**, 123336 (2020).
4. Mahmoud, A. E. D., Stolle, A. & Stelter, M. Sustainable synthesis of high-surface-area graphite oxide via dry ball milling. *ACS Sustain. Chem. Eng.* **6**, 25 (2018).
5. Mellinas, C., Jiménez, A. & del Carmen Garrigós, M. Microwave-assisted green synthesis and antioxidant activity of selenium nanoparticles using theobroma cacao. I. bean shell extract. *Molecules* **24**, 25 (2019).
6. Ahmed, S., Saifullah, A. M., Swami, B. L. & Ikram, S. Green synthesis of silver nanoparticles using *Azadirachta indica* aqueous leaf extract. *J. Radiat. Res. Appl. Sci.* **9**, 25 (2016).
7. Ebadi, M. *et al.* A bio-inspired strategy for the synthesis of zinc oxide nanoparticles (ZnO NPs) using the cell extract of cyanobacterium: *Nostoc sp EA03*: From biological function to toxicity evaluation. *RSC Adv.* **9**, 25 (2019).
8. Mahmoud, A. E. D. & Fawzy, M. Nanosensors and nanobiosensors for monitoring the environmental pollutants. *Top. Min. Metallurg. Mater. Eng.* https://doi.org/10.1007/978-3-030-68031-2_9 (2021).
9. Mousavi, S. M. *et al.* Green synthesis of silver nanoparticles toward bio and medical applications: Review study. *Artif. Cells Nanomed. Biotechnol.* **46**, 3. <https://doi.org/10.1080/21691401.2018.1517769> (2018).
10. Hussain, I., Singh, N. B., Singh, A., Singh, H. & Singh, S. C. Green synthesis of nanoparticles and its potential application. *Biotechnol. Lett.* **38**, 25. <https://doi.org/10.1007/s10529-015-2026-7> (2016).
11. Singh, P., Kim, Y. J., Zhang, D. & Yang, D. C. Biological synthesis of nanoparticles from plants and microorganisms. *Trends Biotechnol.* **34**, 25. <https://doi.org/10.1016/j.tibtech.2016.02.006> (2016).
12. Nilavukkarasi, M., Vijayakumar, S. & Prathipkumar, S. Capparis zeylanica mediated bio-synthesized ZnO nanoparticles as antimicrobial, photocatalytic and anti-cancer applications. *Mater. Sci. Energy Technol.* **3**, 25 (2020).
13. Hussain, A. *et al.* Biogenesis of ZnO nanoparticles using: *Pandanus odorifer* leaf extract: Anticancer and antimicrobial activities. *RSC Adv.* **9**, 25 (2019).
14. Mohamed Isa, E. D., Shamel, K., Che Jusoh, N. W., Mohamad Sukri, S. N. A. & Ismail, N. A. Variation of green synthesis techniques in fabrication of zinc oxide nanoparticles—a mini review. *IOP Conf. Ser. Mater. Sci. Eng.* **1051**, 25 (2021).
15. Loganathan, S., Shivakumar, M. S., Karthi, S., Nathan, S. S. & Selvam, K. Metal oxide nanoparticle synthesis (ZnO-NPs) of *Knoxia sumatrensis* (Retz.) DC. Aqueous leaf extract and its evaluation of their antioxidant, anti-proliferative and larvicidal activities. *Toxicol. Rep.* **8**, 25 (2021).
16. Mahmoud, A. E. D., El-Maghrabi, N., Hosny, M. & Fawzy, M. Biogenic synthesis of reduced graphene oxide from *Ziziphus spina-christi* (Christ's thorn jujube) extracts for catalytic, antimicrobial, and antioxidant potentialities. *Environ. Sci. Pollut. Res.* **20**, 1–16 (2022).
17. Ahmar Rauf, M., Oves, M., Ur Rehman, F., Rauf Khan, A. & Husain, N. Bougainvillea flower extract mediated zinc oxide's nanomaterials for antimicrobial and anticancer activity. *Biomed. Pharmacother.* **116**, 25 (2019).
18. Chabattula, S. C. *et al.* Anticancer therapeutic efficacy of biogenic Am-ZnO nanoparticles on 2D and 3D tumor models. *Mater. Today Chem.* **22**, 25 (2021).
19. Berehu, H. M. *et al.* Cytotoxic potential of biogenic zinc oxide nanoparticles synthesized from *Swertia chirayita* leaf extract on colorectal cancer cells. *Front. Bioeng. Biotechnol.* **9**, 25 (2021).
20. Khezri, K., Saeedi, M. & Maleki Dizaj, S. Application of nanoparticles in percutaneous delivery of active ingredients in cosmetic preparations. *Biomed. Pharmacother.* **106**, 25. <https://doi.org/10.1016/j.biopha.2018.07.084> (2018).
21. Smijs, T. G. & Pavel, S. Titanium dioxide and zinc oxide nanoparticles in sunscreens: Focus on their safety and effectiveness. *Nanotechnol. Sci. Appl.* **4**, 25. <https://doi.org/10.2147/nsa.s19419> (2011).
22. Nasrollahzadeh, M. S. *et al.* Zinc oxide nanoparticles as a potential agent for antiviral drug delivery development: A systematic literature review. *Curr. Nanosci.* **18**, 25 (2021).
23. Perera, W. P. T. D. *et al.* Albumin grafted coaxial electrosprayed polycaprolactone-zinc oxide nanoparticle for sustained release and activity enhanced antibacterial drug delivery. *RSC Adv.* **12**, 25 (2022).
24. Shalaby, M. A., Anwar, M. M. & Saeed, H. Nanomaterials for application in wound healing: Current state-of-the-art and future perspectives. *J. Polym. Res.* **29**, 25. <https://doi.org/10.1007/s10965-021-02870-x> (2022).
25. Kaushik, M. *et al.* Investigations on the antimicrobial activity and wound healing potential of ZnO nanoparticles. *Appl. Surf. Sci.* **479**, 25 (2019).
26. Espitia, P. J. P., Otoni, C. G. & Soares, N. F. F. Zinc oxide nanoparticles for food packaging applications. *Antimicrob. Food Packag.* <https://doi.org/10.1016/B978-0-12-800723-5.00034-6.4> (2016).

27. Doan Thi, T. U. *et al.* Green synthesis of ZnO nanoparticles using orange fruit peel extract for antibacterial activities. *RSC Adv.* **10**, 25 (2020).
28. Shobha, N. *et al.* Synthesis and characterization of Zinc oxide nanoparticles utilizing seed source of *Ricinus communis* and study of its antioxidant, antifungal and anticancer activity. *Mater. Sci. Eng. C* **97**, 25 (2019).
29. Zahran, M. A. & Willis, A. J. The vegetation of Egypt. *Plant Veget.* **2**, 25 (2009).
30. El-Borady, O. M., Fawzy, M. & Hosny, M. Antioxidant, anticancer and enhanced photocatalytic potentials of gold nanoparticles biosynthesized by common reed leaf extract. *Appl. Nanosci. (Switzerland)* <https://doi.org/10.1007/s13204-021-01776-w> (2021).
31. Hosny, M., Fawzy, M., Abdelfatah, A. M., Fawzy, E. E. & Eltaweil, A. S. Comparative study on the potentialities of two halophytic species in the green synthesis of gold nanoparticles and their anticancer, antioxidant and catalytic efficiencies. *Adv. Powder Technol.* **32**, 25 (2021).
32. Vijayakumar, S. *et al.* *Acalypha fruticosa* L. Leaf extract mediated synthesis of ZnO nanoparticles: Characterization and antimicrobial activities. *Mater. Today Proc.* **23**, 25 (2019).
33. Fatimah, I., Pradita, R. Y. & Nurfalinda, A. Plant extract mediated of ZnO nanoparticles by using ethanol extract of mimosa pudica leaves and coffee powder. *Proced. Eng.* **148**, 25 (2016).
34. Heneidy, S. Z. & Bidak, L. M. Potential uses of plant species of the coastal mediterranean region, Egypt. *Pak. J. Biol. Sci.* **7**, 1010–1023 (2004).
35. Manousaki, E. & Kalogerakis, N. Halophytes present new opportunities in phytoremediation of heavy metals and saline soils. *Ind. Eng. Chem. Res.* **50**, 25 (2011).
36. Zengin, G., Aumeeruddy-Elalfi, Z., Mollica, A., Yilmaz, M. A. & Mahomoodally, M. F. In vitro and in silico perspectives on biological and phytochemical profile of three halophyte species—a source of innovative phytopharmaceuticals from nature. *Phytomedicine* **38**, 35–44 (2018).
37. Xin, P. *et al.* Surface water and groundwater interactions in salt marshes and their impact on plant ecology and coastal biogeochemistry. *Rev. Geophys.* **60**, 5. <https://doi.org/10.1029/2021RG000740> (2022).
38. International Union for Conservation of Nature. *International Union for Conservation of Nature Natural Resources IUCN Red List Categories and Criteria* (IUCN, 2001).
39. Boulos, L. *Flora of Egypt* Vol 417 21–22 (Al Hadara Publishing, 1999).
40. Safawo, T., Sandeep, B. V., Pola, S. & Tadesse, A. Synthesis and characterization of zinc oxide nanoparticles using tuber extract of ancho (*Coccoloba abyssinica* (Lam.) Cong.) for antimicrobial and antioxidant activity assessment. *Open Nano* **3**, 25 (2018).
41. Soltanian, S. *et al.* Biosynthesis of zinc oxide nanoparticles using hertia intermedia and evaluation of its cytotoxic and antimicrobial activities. <https://doi.org/10.1007/s12668-020-00816-z/Published>.
42. Ogbolo, O. O., Segun, P. A. & Adeniji, A. J. In vitro cytotoxic activity of medicinal plants from Nigeria ethnomedicine on Rhabdomyosarcoma cancer cell line and HPLC analysis of active extracts. *BMC Complement Altern. Med.* **17**, 25 (2017).
43. Slater, T. F., Sawyer, B. & Sträuli, U. Studies on succinate-tetrazolium reductase systems. III Points of coupling of four different tetrazolium salts. *Biochim. Biophys. Acta* **77**, 25 (1963).
44. Alley, M. C. *et al.* Feasibility of drug screening with panels of human tumor cell lines using a microculture tetrazolium assay. *Cancer Res.* **48**, 25 (1988).
45. van de Loosdrecht, A. A., Beelen, R. H. J., Ossenkuppe, G. J., Broekhoven, M. G. & Langenhuijsen, M. M. A. C. A tetrazolium-based colorimetric MTT assay to quantitate human monocyte mediated cytotoxicity against leukemic cells from cell lines and patients with acute myeloid leukemia. *J. Immunol. Methods* **174**, 25 (1994).
46. Gonelimali, F. D. *et al.* Antimicrobial properties and mechanism of action of some plant extracts against food pathogens and spoilage microorganisms. *Front. Microbiol.* **9**, 25 (2018).
47. Aldalbahi, A. *et al.* Greener synthesis of zinc oxide nanoparticles: Characterization and multifaceted applications. *Molecules* **25**, 25 (2020).
48. López-Cuenca, S. *et al.* High-yield synthesis of zinc oxide nanoparticles from bicontinuous microemulsions. *J. Nanomater.* **2011**, 25 (2011).
49. Sajadi, S. M. *et al.* Natural iron ore as a novel substrate for the biosynthesis of bioactive-stable ZnO@CuO@iron ore NCs: A magnetically recyclable and reusable superior nanocatalyst for the degradation of organic dyes, reduction of Cr(vi) and adsorption of crude oil aromatic compounds, including PAHs. *RSC Adv.* **8**, 62. <https://doi.org/10.1039/c8ra06028b> (2018).
50. Meena, P. L., Poswal, K. & Surela, A. K. Facile synthesis of ZnO nanoparticles for the effective photodegradation of malachite green dye in aqueous solution. *Water Environ. J.* **36**, 25 (2022).
51. El-Belely, E. F. *et al.* Green synthesis of zinc oxide nanoparticles (ZnO-nps) using arthrospira platensis (class: Cyanophyceae) and evaluation of their biomedical activities. *Nanomaterials* **11**, 25 (2021).
52. Faye, G., Jebessa, T. & Wubalem, T. Biosynthesis, characterisation and antimicrobial activity of zinc oxide and nickel doped zinc oxide nanoparticles using *Euphorbia abyssinica* bark extract (2021). <https://doi.org/10.1049/nbt2.12072>.
53. Dulta, K., Koşarsoy Ağçeli, G., Chauhan, P., Jasrotia, R. & Chauhan, P. K. A novel approach of synthesis zinc oxide nanoparticles by *Bergenia ciliata* rhizome extract: Antibacterial and anticancer potential. *J. Inorg. Organomet. Polym. Mater.* **31**, 25 (2021).
54. Faisal, S. *et al.* Green synthesis of zinc oxide (ZnO) nanoparticles using aqueous fruit extracts of *Myristica fragrans*: Their characterizations and biological and environmental applications. *ACS Omega* **6**, 25 (2021).
55. Adams, R. P. Identification of essential oil components by gas chromatography/mass spectrometry. *J. Am. Soc. Mass Spectrometry* **8**, 25 (2007).
56. VStein, S., Mirokhin, D., Tchekhovskoi, D., & Nist, G. M. The NIST Mass Spectral Search Program for the NIST/EPA/NIH Mass Spectra Library. Gaithersburg, MD: Standard Reference Data Program of the National Institute of Standards and Technology (2002).
57. Mahmoud, A. E. D., Hosny, M., El-Maghrabi, N. & Fawzy, M. Facile synthesis of reduced graphene oxide by Tecoma stans extracts for efficient removal of Ni (II) from water: Batch experiments and response surface methodology. *Sustain. Environ. Res.* **32**, 25 (2022).
58. Balasubramani, G. *et al.* GC-MS analysis of bioactive components and synthesis of gold nanoparticle using *Chloroxylon swietenia* DC leaf extract and its larvicidal activity. *J. Photochem. Photobiol. B* **148**, 25 (2015).
59. Barzinjy, A. A. & Azeez, H. H. Green synthesis and characterization of zinc oxide nanoparticles using *Eucalyptus globulus* Labill. leaf extract and zinc nitrate hexahydrate salt. *SN Appl. Sci.* **2**, 25 (2020).
60. Anitha, R., Ramesh, K. V., Ravishankar, T. N., Sudheer Kumar, K. H. & Ramakrishnappa, T. Cytotoxicity, antibacterial and antifungal activities of ZnO nanoparticles prepared by the *Artocarpus gomezianus* fruit mediated facile green combustion method. *J. Sci. Adv. Mater. Devices* **3**, 25 (2018).
61. Chandra, H., Patel, D., Kumari, P., Jangwan, J. S. & Yadav, S. Phyto-mediated synthesis of zinc oxide nanoparticles of *Berberis aristata*: Characterization, antioxidant activity and antibacterial activity with special reference to urinary tract pathogens. *Mater. Sci. Eng. C* **102**, 25 (2019).
62. Majeed, S., Danish, M., Ismail, M. H., Ansari, M. T. & Ibrahim, M. N. M. Anticancer and apoptotic activity of biologically synthesized zinc oxide nanoparticles against human colon cancer HCT-116 cell line- in vitro study. *Sustain. Chem. Pharm.* **14**, 25 (2019).
63. Miri, A., Khatami, M., Ebrahimi, O. & Sarani, M. Cytotoxic and antifungal studies of biosynthesized zinc oxide nanoparticles using extract of *Prosopis farcta* fruit. *Green Chem. Lett. Rev.* **13**, 25. <https://doi.org/10.1080/17518253.2020.1717005> (2020).

64. Ahamed, M., Akhtar, M. J., Khan, M. A. M. & Alhadlaq, H. A. Enhanced anticancer performance of eco-friendly-prepared Mo-ZnO/RGO nanocomposites: Role of oxidative stress and apoptosis. *ACS Omega* **7**, 25 (2022).
65. Al-Mohaimed, A. M., Al-Onazi, W. A. & El-Tohamy, M. F. Multifunctional eco-friendly synthesis of ZnO nanoparticles in biomedical applications. *Molecules* **27**, 25 (2022).
66. Schreyer, M., Guo, L., Thirunahari, S., Gao, F. & Garland, M. Simultaneous determination of several crystal structures from powder mixtures: The combination of powder X-ray diffraction, band-target entropy minimization and Rietveld methods. *J. Appl. Crystallogr.* **47**, 25 (2014).
67. Pu, Y., Niu, Y., Wang, Y., Liu, S. & Zhang, B. Statistical morphological identification of low-dimensional nanomaterials by using TEM. *Particuology* **61**, 11–17 (2022).
68. Wu, C. M., Baltrusaitis, J., Gillan, E. G. & Grassian, V. H. Sulfur dioxide adsorption on ZnO nanoparticles and nanorods. *J. Phys. Chem. C* **115**, 10164–10172 (2011).
69. Saranya, S., Vijayanarai, K., Pavithra, S., Raihana, N. & Kumanan, K. In vitro cytotoxicity of zinc oxide, iron oxide and copper nanopowders prepared by green synthesis. *Toxicol. Rep.* **4**, 25 (2017).
70. Chelladurai, M. *et al.* Anti-skin cancer activity of *Alpinia calcarata* ZnO nanoparticles: Characterization and potential antimicrobial effects. *J Drug Deliv. Sci. Technol.* **61**, 102180 (2021).
71. Lingaraju, K., Naika, H. R., Nagabhushana, H. & Nagaraju, G. *Euphorbia heterophylla* (L.) mediated fabrication of ZnO NPs: Characterization and evaluation of antibacterial and anticancer properties. *Biocatal. Agric. Biotechnol.* **18**, 25 (2019).
72. Sana, S. S. *et al.* *Crotalaria verrucosa* leaf extract mediated synthesis of zinc oxide nanoparticles: Assessment of antimicrobial and anticancer activity. *Molecules* **25**, 25 (2020).
73. Bishit, G. & Rayamajhi, S. ZnO nanoparticles: A promising anticancer agent. *Nanobiomedicine* <https://doi.org/10.5772/63437> (2016).
74. Bharath, B., Perinbam, K., Devanesan, S., AlSalhi, M. S. & Saravanan, M. Evaluation of the anticancer potential of Hexadecanoic acid from brown algae *Turbinaria ornata* on HT–29 colon cancer cells. *J. Mol. Struct.* **1235**, 25 (2021).
75. Selim, Y. A., Azb, M. A., Ragab, I., Abd El-Azim, H. M. & M., Green synthesis of zinc oxide nanoparticles using aqueous extract of *Deverra tortuosa* and their cytotoxic activities. *Sci. Rep.* **10**, 25 (2020).
76. Medini, F. *et al.* Phytochemical analysis, antioxidant, anti-inflammatory, and anticancer activities of the halophyte *Limonium densiflorum* extracts on human cell lines and murine macrophages. *South Afr. J. Bot.* **99**, 25 (2015).
77. Pan, M. H., Ghai, G. & Ho, C. T. Food bioactives, apoptosis, and cancer. *Mol. Nutr. Food Res.* **52**, 20. <https://doi.org/10.1002/mnfr.200700380> (2008).
78. Abdallah, H. M. & Ezzat, S. M. Effect of the method of preparation on the composition and cytotoxic activity of the essential oil of *Pituranthos tortuosus*. *Z. Nat. Sect. C J. Biosci.* **66 C**, 25 (2011).
79. Iqbal, J. *et al.* Green synthesis of zinc oxide nanoparticles using *Elaeagnus angustifolia* L. leaf extracts and their multiple in vitro biological applications. *Sci. Rep.* **11**, 25 (2021).
80. Norouzi Jobie, F., Ranjbar, M., Hajizadeh Moghaddam, A. & Kiani, M. Green synthesis of zinc oxide nanoparticles using *Amygdalus scoparia* Spach stem bark extract and their applications as an alternative antimicrobial, anticancer, and anti-diabetic agent. *Adv. Powder Technol.* **32**, 21 (2021).
81. Chen, F. C., Huang, C. M., Yu, X. W. & Chen, Y. Y. Effect of nano zinc oxide on proliferation and toxicity of human gingival cells. *Hum. Exp. Toxicol.* **41**, 15 (2022).
82. Sajjad, A. *et al.* Photoinduced fabrication of zinc oxide nanoparticles: Transformation of morphological and biological response on light irradiance. *ACS Omega* **6**, 75 (2021).
83. Sohail, M. F. *et al.* Green synthesis of zinc oxide nanoparticles by neem extract as multi-facet therapeutic agents. *J. Drug Deliv. Sci. Technol.* **59**, 15 (2020).
84. Lopes, M., Sanches-Silva, A., Castilho, M., Cavaleiro, C. & Ramos, F. Halophytes as source of bioactive phenolic compounds and their potential applications. *Crit. Rev. Food Sci. Nutr.* **20**, 20. <https://doi.org/10.1080/10408398.2021.1959295> (2021).
85. Bouarab-Chibane, L. *et al.* Antibacterial properties of polyphenols: Characterization and QSAR (quantitative structure–activity relationship) models. *Front. Microbiol.* **10**, 77 (2019).
86. Guimarães, A. C. *et al.* Antibacterial activity of terpenes and terpenoids present in essential oils. *Molecules* **24**, 11 (2019).
87. Sirelkhatim, A. *et al.* Review on zinc oxide nanoparticles: Antibacterial activity and toxicity mechanism. *Nano-Micro Lett.* **7**, 219–242. <https://doi.org/10.1007/s40820-015-0040-x> (2015).
88. Singh, T. A. *et al.* A state of the art review on the synthesis, antibacterial, antioxidant, antidiabetic and tissue regeneration activities of zinc oxide nanoparticles. *Adv. Coll. Interface Sci.* **295**, 25. <https://doi.org/10.1016/j.cis.2021.102495> (2021).
89. Gao, Y. *et al.* Biofabrication of zinc oxide nanoparticles from *Aspergillus niger*, their antioxidant, antimicrobial and anticancer activity. *J. Clust. Sci.* **30**, 11 (2019).
90. Luo, Q. *et al.* Terpenoid composition and antioxidant activity of extracts from four chemotypes of *Cinnamomum camphora* and their main antioxidant agents. *Biofuels Bioprod. Biorefin.* **16**, 510–522 (2022).
91. Bose, J., Rodrigo-Moreno, A. & Shabala, S. ROS homeostasis in halophytes in the context of salinity stress tolerance. *J. Exp. Bot.* **65**, 25. <https://doi.org/10.1093/jxb/ert430> (2014).

Acknowledgements

The authors would like to thank the support of Egyptian Science, Technology, and Innovation Funding Authority (STIFA) for the grant number 45888 under the umbrella of USAID/STDF collaboration project as well as the support of Egyptian Academy of Scientific Research and Technology for the SA-Egypt Joint Project number 7981.

Author contributions

B.N.: investigation, methodology, formal analysis, visualization, writing—original draft preparation. M.F.: conceptualization, methodology, investigation, funding acquisition, resources, project administration, review and editing. M.W.A.H.: conceptualization, investigation, fieldwork, species collection, identification, review and editing. A.E.D.M.: methodology, visualization, formal analysis, writing—original draft preparation, review and editing.

Funding

Open access funding provided by The Science, Technology & Innovation Funding Authority (STDF) in cooperation with The Egyptian Knowledge Bank (EKB).

Competing interests

The authors declare no competing interests.

Additional information

Supplementary Information The online version contains supplementary material available at <https://doi.org/10.1038/s41598-022-24805-2>.

Correspondence and requests for materials should be addressed to B.N.

Reprints and permissions information is available at www.nature.com/reprints.

Publisher's note Springer Nature remains neutral with regard to jurisdictional claims in published maps and institutional affiliations.



Open Access This article is licensed under a Creative Commons Attribution 4.0 International License, which permits use, sharing, adaptation, distribution and reproduction in any medium or format, as long as you give appropriate credit to the original author(s) and the source, provide a link to the Creative Commons licence, and indicate if changes were made. The images or other third party material in this article are included in the article's Creative Commons licence, unless indicated otherwise in a credit line to the material. If material is not included in the article's Creative Commons licence and your intended use is not permitted by statutory regulation or exceeds the permitted use, you will need to obtain permission directly from the copyright holder. To view a copy of this licence, visit <http://creativecommons.org/licenses/by/4.0/>.

© The Author(s) 2022